

OBSERVATIONAL STUDIES OF INTERMEDIATE-MASS PROTOSTARS WITH PDBI, 30M, AND HERSCHEL

T. Alonso-Albi¹ and A. Fuente¹

Abstract. The study of intermediate-mass (IM) protostars is important because they provide the link between low-mass and high-mass star formation mechanisms, which are different and not well understood. To advance towards the comprehension of high-mass objects IM protostars are the next natural step. IM and high mass protostars are usually too far to be studied in detail, and their rapid evolution while they are still embedded in the parent cloud makes high-resolution radioastronomy (interferometry) a must. This work shows the most relevant results achieved by our group in the study of circumstellar disks and envelopes around IM protostars during the last few years, using IRAM instruments (30 m radiotelescope at Spain and *Plateau de Bure* interferometer in France) and the NRAO's *Very Large Array* (VLA) interferometer at USA.

Keywords: star formation, pre-main-sequence, intermediate-mass protostars, protoplanetary disks

1 Introduction

IM protostars are objects between 3 and 8 M_{\odot} . We can differentiate two groups of IM protostars: those between 3 and 5 M_{\odot} (the so called Herbig Ae stars, HAe hereafter), and those between 5 and 8 M_{\odot} (Herbig Be stars, HBe hereafter). The formation of HAe stars shows similarities with low-mass or T Tauri stars. In fact, in these objects the mass accretion phase of the protostar occurs prior to (and independently from) its contraction towards the main sequence. The relatively slow evolution during some tenths of million years simplify the study of these objects, since they soon disperse the parent cloud and become visible. In contrast, HBe protostars are usually found in clusters, highly embedded in massive and chemically complex molecular clouds. Their accretion and contraction phases coexist simultaneously, affecting the physical properties and the chemistry of the surrounding circumstellar disk and envelope in much lower time-scales. Even in a sample of (apparently) similar HBe objects we could have each of them at different evolutionary status and evolving with different rates. Since the sample of HBe stars is scarce compared to the HAe or T Tauri ones, the study and comprehension of HBe stars is not easy, but the sensitivity of the instrumentation available today is making this goal feasible.

Our aim is the study of the chemistry in envelopes around IM class 0 protostars, which are the youngest objects detectable at millimeter (mm) wavelengths and where there are still few studies. In more evolved objects (HBe stars that have eroded the cloud to become visible) we are also interested in the properties of their circumstellar disks and the differences between these disks and those around T Tauri stars. The detection frequency, chemistry, and physical properties (mass, size, and grain population) are expected to be different mainly due to the intense UV radiation field (with the contribution of the surrounding objects since clustering is a common phenomenon in IM protostars) and the variability of the central source.

As an aid for the analysis and comprehension of the observations described in the next two sections we developed new tools and models*. We will emphasize two of them that have been used actively in our work: a radiative transfer model that can operate in LTE and slab LVG approximations, and an implementation of the circumstellar disk model by Dullemond et al. (2001).

¹ Observatorio Astronómico Nacional (OAN), Apdo. 112, E-28800 Alcalá de Henares, Madrid. e-mail: t.alonso@oan.es. Presentation available at <http://conga.oan.es/%7Ealonso/sources/presentationSF2A.pdf>.

*Our programs can be installed for any operating system at <http://conga.oan.es/%7Ealonso/doku.php?id=jparsec>. Source code is included and released under GPL license.

2 Observations of envelopes around IM protostars

Continuum observations, coupled with molecular line spectra, allowed us to study the physical and chemical structure of a sample of five IM class 0 protostars (Cep E-mm, Serpens-FIRS 1, CB3, IC1396-N, NGC 7129-FIRS 2). We also observed for comparison the more evolved class I sources S140 and LkH α 234 (see Fig. 1). Crimier et al. (2010) derived the temperature-density profiles based on the SED and the SCUBA maps at 450 μm and 850 μm . Adopting these profiles, Alonso-Albi et al. (2010) modeled the chemistry of these envelopes to fit the radial distribution of the integrated intensity emission of the C ^{18}O 1 \rightarrow 0, N $_2\text{H}^+$ 1 \rightarrow 0 and N $_2\text{D}^+$ 2 \rightarrow 1 lines observed with the IRAM 30 m telescope.

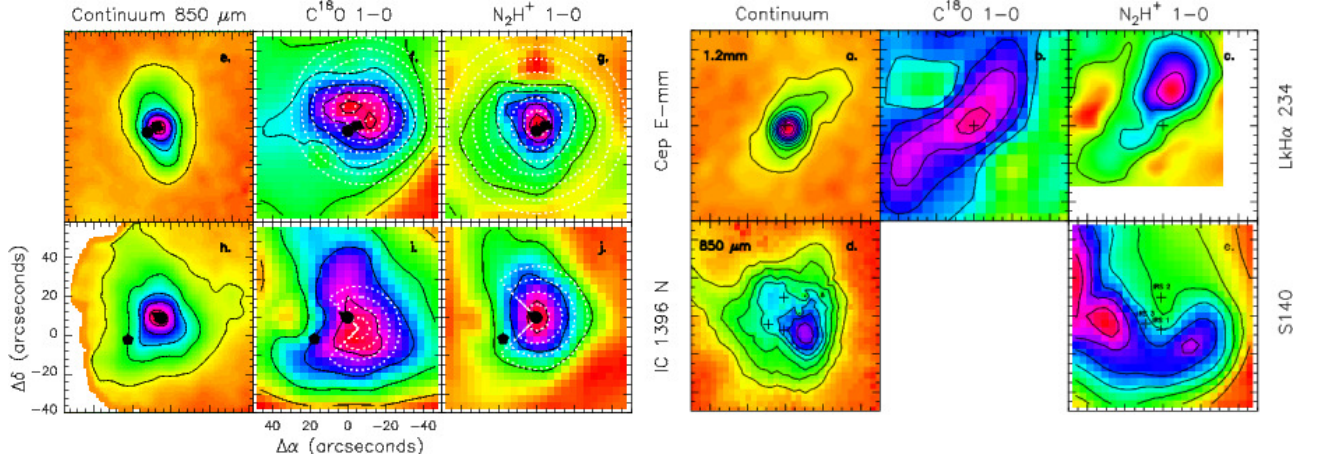


Fig. 1. Left: Observations of C ^{18}O and N $_2\text{H}^+$ towards two of the IM class 0 protostars. White dotted lines represent the different rings considered to obtain the integrated intensity profiles to compare observations and models for different molecules and sources. **Right:** The same observations towards class I objects.

We fitted the radial distribution of the C ^{18}O emission in two steps. First, the C ^{18}O abundance profile is calculated using the chemical code originally described in Caselli et al. (2002), and later updated by Caselli et al. (2008) to include new measurements of the CO and N $_2$ binding energies (Collings et al. 2003; Öberg et al. 2005) and sticking coefficients (Bisschop et al. 2006), and thermal desorption. The density-temperature profiles obtained by Crimier et al. (2010) were used as the physical basis for the chemical model. Once the C ^{18}O abundance profile is derived, we used our radiative transfer model to obtain the emission predicted with this abundance profile to compare with the C ^{18}O observations.

In the standard model (model 1 in Fig. 2), the C ^{18}O abundance decreases inwards the protostellar envelope because of the CO depletion onto grain mantles until the gas and dust reach the CO evaporation temperature, $\approx 20\text{-}25$ K, where the CO is released back to the gas phase and the C ^{18}O abundance sharply increases to $1.6 \cdot 10^{-7}$. Surprisingly, the standard model failed to reproduce the integrated intensity maps of all the IMs. This model assumes that the CO has a binding energy of 1100 K, compatible with CO depleted in a CO-CO matrix. Model 2 assumes a binding energy a 5000 K, compatible with a CO-H $_2\text{O}$ matrix. The radial intensity profiles obtained with both models for C ^{18}O (see first and second panels in the middle in Fig. 2) show that model 1 is more consistent than model 2, so we started from model 1 and we modified it to reduce the C ^{18}O emission in the inner region of the envelope. In three of the sources, NGC 7129-FIRS 2, Cep E-mm and CB3, the C ^{18}O abundance needed to be decreased by a factor of 10 within the CO evaporation region ($T_k > 25$ K) to fit the observations (model 3), both in the absolute values of the integrated intensities and in the slopes of the profiles. These sources were also those with the higher deuterium fractionation, $[\text{N}_2\text{D}^+]/[\text{N}_2\text{H}^+] > 0.01$, and presumably the youngest in our sample. This CO deficiency was interpreted as possible evidence for an active surface chemistry in the protostellar envelope, where CO is efficiently converted in more complex organic molecules, such as CH $_3\text{OH}$. In the other two, Serpens FIRS 1 and IC 1396 N, the observations were fitted by decreasing the C ^{18}O abundance by the same factor but only in the hot core region, $T_k > 100$ K (model 4). In these sources $[\text{N}_2\text{D}^+]/[\text{N}_2\text{H}^+] < 0.01$, and the low C ^{18}O abundance was interpreted to be due to photodissociation. Our results, however, suffered from the limited spatial resolution of the 30 m telescope. Moreover, we were observing low excitation lines whose emission could be dominated by the external part of the envelope, so additional observations of high excitation lines were required to confirm this result.

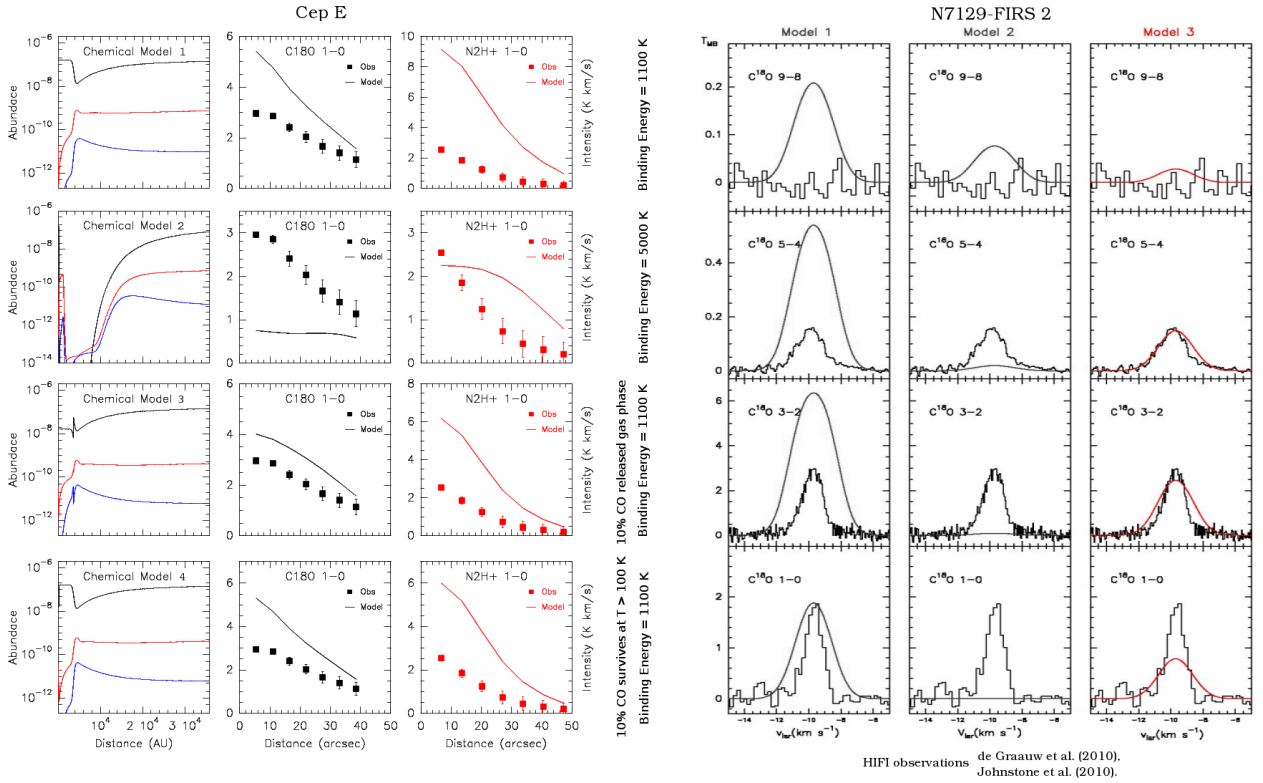


Fig. 2. Left: Sequence of chemical models applied to Cep E until a reasonably fit to observations was found with model 3, that assumes only 10% of CO is released back to gas phase in the inner region ($T > 25$ K). Model 4 assumes that only 10% of CO is not photodissociated in the hot core ($T > 100$ K), and this model was more consistent with observations for IC1396-N and Serpens-FIRS 1. **Right:** Observations and model results of high J CO transitions for NGC 7129-FIRS 2. Model 3 is confirmed to be the most consistent, with some contribution of the cloud to 1 \rightarrow 0 transition.

For the first time, Herschel provided the opportunity to observe the high excitation lines of CO (and isotopes) towards young stellar objects. Combining ground based observations of the C¹⁸O J=1 \rightarrow 0 and J=3 \rightarrow 2 lines with the Herschel/HIFI (de Graauw et al. 2010; Johnstone et al. 2010) observations of the C¹⁸O J=5 \rightarrow 4 line and J=9 \rightarrow 8 line, Fuente et al. (2011, in preparation) derived the C¹⁸O abundance profile across the envelope of the young IM protostar NGC 7129-FIRS 2. The new observations proves that the C¹⁸O abundance is $\sim 1.6 \cdot 10^{-8}$ in the inner region of the envelope, corroborating previous results by Alonso-Albi et al. (2010).

3 Observations of circumstellar disks

We carried observations at mm wavelengths in a sample of Herbig Ae/Be stars. In the HBe star R Mon we obtained high angular resolution observations in the continuum and in the ¹²CO 1 \rightarrow 0 and 2 \rightarrow 1 rotational lines, using the A⁺ configuration of the *Plateau de Bure* interferometer (PdBI) (Fuente et al. 2006). At 1.3 mm the resolution reached 0.7x0.3'', allowing us to detect the gas rotating around R Mon in molecular lines. We modeled the disk in molecular lines using our radiative transfer model, and found compatible models for a flared and a flat geometry. With this modeling we also estimated dynamically the mass of R Mon itself in 8 M_⊙. Since our ¹²CO lines were optically thick we needed further observations in an optically thin transition to obtain a more detailed look of the geometry of the disk, so we obtained new observations of ¹³CO 1 \rightarrow 0 (Alonso-Albi et al. 2007). In Fuente et al. (2006) we concluded that the flat geometry was more probable, since the mass of the disk derived from the model was in very good agreement with the mass estimated from the (optically thin) mm continuum observations. In Alonso-Albi et al. (2007) we confirmed this result, since we tentatively detected ¹³CO towards R Mon with the expected intensity for a dusty disk of 0.001 M_⊙ (right panel in Fig. 3). The expected result for a flared disk was eight times this value.

The HAe star VV Ser was also observed (Alonso-Albi et al. 2008) with the PdBI in its B configuration, and with the VLA in its D configuration at 44, 22, and 8 GHz (0.7, 1.3, and 3.5 cm). We detected continuum emission

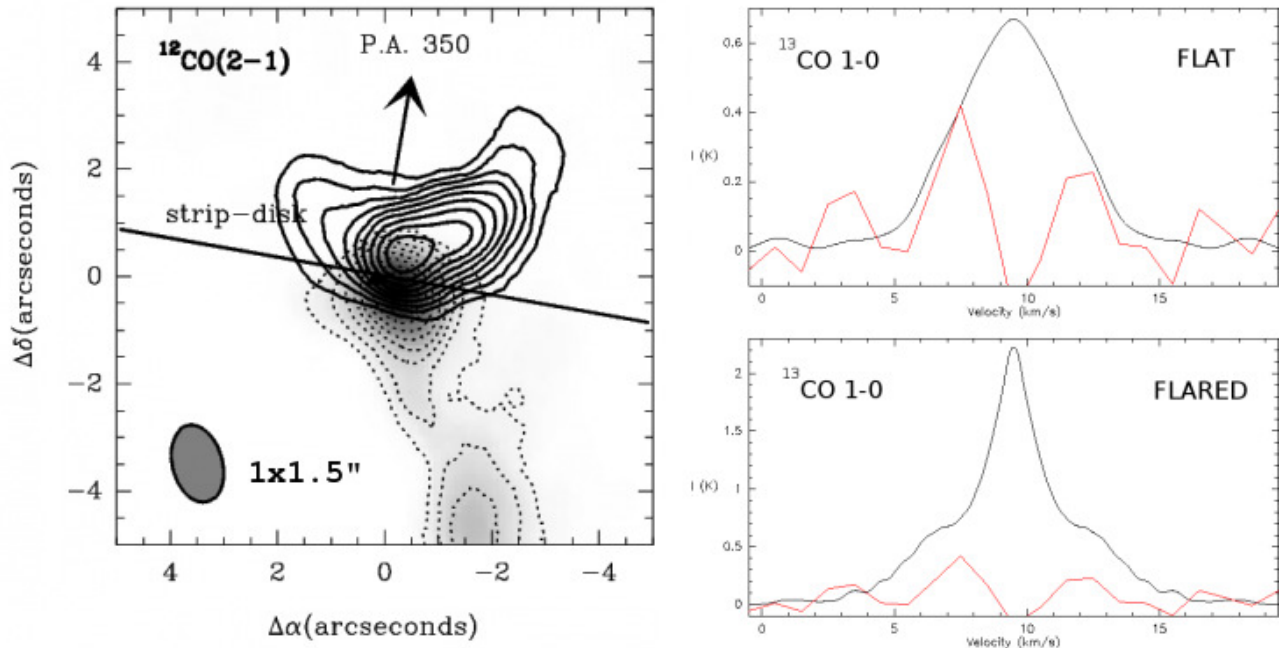


Fig. 3. Left: $^{12}\text{CO}(2\rightarrow 1)$ observations towards R Mon, with the direction of the outflow and the expected direction of the major axis of the circumstellar disk superimposed. The contours of the emission are separated in a blueshifted component (north) and a redshifted one (south, dotted lines). **Right:** $^{13}\text{CO}(1\rightarrow 0)$ observations towards R Mon (red), with the predicted intensity from the flared and flat geometries (black). To become optically thick the disk is eight times more massive in the flared model and therefore it predicts an intensity which is inconsistent with observations (Alonso-Albi et al. 2007).

with the PdBI at 1.3 and 2.6 mm, and tentatively with VLA at 7 mm. We did not detect continuum emission at 1.3 or 3.5 cm, neither molecular (^{12}CO) emission. We used our observations and those from Pontoppidan et al. (2007) to complete the SED and we modeled it using our implementation of the Dullemond et al. (2001) circumstellar disk model. We found a disk with an outer radius of only 40 AU, and a mass of dust of $4 \cdot 10^{-5} M_{\odot}$ [†]. This compact and light disk is not usual around low mass objects, where disks usually reach sizes greater than 100 AU. This result and the lack of CO emission was interpreted to be due to the high number of IR sources present around this source (24 in a radius of 0.2 pc according to Testi et al. 1998), that could be responsible of the photoevaporation of the outer part of the disk. The main conclusion of this work was the presence of grains with a maximum size close to 1 cm in the midplane. This result is supported by the flat shape of the SED between 1 and 3 mm, with a spectral index of 0.9. A spectral index below 1 is indicative of grains with a maximum size of 3 mm or larger (Draine 2006).

Alonso-Albi et al. (2009) completed a search for circumstellar disks in a sample of six HBe stars: R Mon, MWC 1080, MWC 137, MWC 297, Z CMa, and LkH α 215. We obtained observations from the PdBI at mm wavelengths and from the VLA at cm wavelengths. We also used MIPS and IRS data from Spitzer for MWC 1080, MWC 297, R Mon, and LkH α 215, and completed the SED using continuum photometry from a variety of catalogs (compiled with data from instruments of different resolutions) using Vizier service. We found excess from the expected level of the free-free emission (derived from VLA observations) in the mm fluxes of four out of the six sources in our sample, only MWC 137 and LkH α 215 showed no trace of a circumstellar disk. A first evident result is that for all HBe sources most of the continuum emission at far IR and sub-mm wavelengths comes from the envelope surrounding the star, so an envelope component must be added to the disk model to account for this flux. As in the case of VV Ser, the spectral index found in these sources was close to unity, which indicates the presence of grains with maximum sizes close to the cm, even for these extremely

[†]Here we specifically mention the *mass of dust* only, in other sections we refer to the *mass of the disk*, which we consider to be 100 times greater due to the gas-to-dust mass ratio.

4 Conclusions

We carried observations in continuum and molecular lines in a sample of six HBe and five HAe stars. We detected a circumstellar disk in six out of the four HBe sources, and in four out of the five HAe ones. The entire SED was modeled with a disk + envelope (always dominant in sub-mm regime in HBe stars) + free-free emission (to determine the spectral index of the SED in mm wavelengths, and the mass of the disks) model.

The youngest sources (R Mon, Z CMa) still show emission in molecular lines. We modeled the disk around R Mon in ^{12}CO 1 \rightarrow 0 and 2 \rightarrow 1, obtaining a direct estimate of its mass assuming Keplerian rotation. ^{13}CO 1 \rightarrow 0 observations showed the disk is flat.

The spectral index of the dust in mm wavelengths is always < 1 in HBe stars, probably due to the presence of a grain population up to 1 cm in size. Since grain growth occurs even in very young HBe sources, this process seems to be independent from the properties (age, mass) of the HBe source. In case this process happens before photoevaporation gets intense planetesimals around HBe stars would be possible.

The mass of the disks (gas+dust) around HBe sources ranges from $0.2 M_{\odot}$ in extremely young sources (Z CMa) to about $0.003 M_{\odot}$ in more evolved sources (MWC 1080 for instance) or lower, with a high dispersion in the values since the dissipation of the disk occurs in very short timescales.

HAe stars in our sample are older, their disks more massive (with an average value of $0.04 M_{\odot}$), and the grains have not reached cm sizes yet. HAe sources between 3 and $5 M_{\odot}$ show evidences that grain growth is happening, although this process is slower compared with HBe sources.

An important problem is the dependency of the mass of the disks with the mass and age of the stars, and with the effects of the objects in the vicinity. ALMA will provide a more representative sample with more objects in each mass range (up to 5 kpc), and will resolve the disks, allowing detailed chemical studies.

References

- Alonso-Albi, T., Fuente, A., Bachiller, R., et al. 2007, arXiv:astro-ph/0702119
 Alonso-Albi, T., Fuente, A., Bachiller, R., et al. 2008, ApJ, 680, 1289
 Alonso-Albi, T., Fuente, A., Bachiller, R., et al. 2009, A&A, 497, 117
 Alonso-Albi, T., Fuente, A., Crimier, N., et al. 2010, A&A, 518, A52+
 Bisschop, S. E., Fraser, H. J., Öberg, K. I., van Dishoeck, E. F., & Schlemmer, S. 2006, A&A, 449, 1297
 Boissier, J., Alonso-Albi, T., Fuente, A., et al. 2011, A&A, 531, A50+
 Caselli, P., Vastel, C., Ceccarelli, C., et al. 2008, A&A, 492, 703
 Caselli, P., Walmsley, C. M., Zucconi, A., et al. 2002, ApJ, 565, 344
 Collings, M. P., Dever, J. W., Fraser, H. J., McCoustra, M. R. S., & Williams, D. A. 2003, ApJ, 583, 1058
 Crimier, N., Ceccarelli, C., Alonso-Albi, T., et al. 2010, ArXiv e-prints
 de Graauw, T., Helmich, F. P., Phillips, T. G., et al. 2010, A&A, 518, L6+
 Draine, B. T. 2006, ApJ, 636, 1114
 Dullemond, C. P., Dominik, C., & Natta, A. 2001, ApJ, 560, 957
 Fuente, A., Alonso-Albi, T., Bachiller, R., et al. 2006, ApJ, 649, L119
 Johnstone, D., Fich, M., McCoey, C., et al. 2010, A&A, 521, L41+
 Öberg, K. I., van Broekhuizen, F., Fraser, H. J., et al. 2005, ApJ, 621, L33
 Pontoppidan, K. M., Dullemond, C. P., Blake, G. A., et al. 2007, ApJ, 656, 980
 Testi, L., Palla, F., & Natta, A. 1998, A&AS, 133, 81